p-ISSN 2089 – 0133 e-ISSN 2477-6416 Indonesian Journal of Applied Physics (IJAP) Vol. 15 No. 1 page 176
URL: https://jurnal.uns.ac.id/ijap/article/view/93950 DOI: https://doi.org/10.13057/ijap.v15i1.93950

INTEGRATION OF ELECTRICAL RESISTIVITY TOMOGRAPHY AND BOREHOLE DATA FOR MAPPING LATERITE-BEDROCK BOUNDARIES IN A NICKEL DEPOSIT, 'PHO' BLOCK, SOUTHEAST SULAWESI

Ipho Amanah Pahlawantika[1], Y.Yatini*[1], Muhammad Arief Wicaksono[2]
[1] Geophysics Engineering, Universitas Pembangunan Nasional Veteran Yogyakarta, Yogyakarta, Indonesia.
[2]PT Aneka Tambang Tbk, Antam Tower Building A, TB.Simatupang Jagakarsa, South Jakarta, Jakarta Indonesia
* jeng_tini@upnyk.ac.id

Received 03-10-2024, Revised 27-02-2025, Accepted 15-04-2025,
Available Online 15-04-2025, Published Regularly April 2025

ABSTRACT

Indonesia has the largest nickel reserves in the world, so proper exploration is crucial to map the potential and utilization of this resource. Exploration of nickel laterite is carried out by mapping the boundaries of the laterite zone and bedrock as a prospect zone for further exploration. One of the methods used is *Electrical Resistivity Tomography* (ERT) combined with drill data. The principle of the ERT method involves injecting electric current into the ground to measure variations in subsurface resistivity. These variations in resistivity are then used to map the lithological distribution. ERT data, used as the primary data source to obtain an inversion model, is combined with inline borehole data, involving a total of 8 ERT lines and 23 borehole data points. The integration of both ERT and borehole data characterizes zones of nickel laterite and bedrock. Nickel laterite zones consist of saprolite and limonite lithology, and there is a saprock zone as a transition between the nickel laterite zone and the bedrock. Research in the "PHO" Block shows that resistivity values range from 10.9 Ωm to 1500 Ωm, divided into four main zones: saprolite (<150 Ωm), limonite (150 -700 Ωm), saprock (700 -1000 Ωm), and bedrock (>1000 Ωm). The nickel laterite zones are primarily composed of the saprolite with high Ni, high weathering, and porous zone, limonite zones with high FeO2 and low conductive material, and saprock zones that are transition zones of the nickel laterite with low weathering, high fracture, and bedrock. The boundary between the laterite zone and bedrock is predominantly found at depths ranging from 31.1 meters to over 49.9 meters, indicating the presence of bedrock. The limonite zones, which accumulate to more than 20 meters in thickness, are evenly distributed, with lower accumulations in the south and northeast. Thinner saprolite zones were found at depths exceeding 20 meters, while saprock and bedrock were detected starting from a depth of 13.4 meters and extending to over 49.9 meters. The integration of the ERT method and borehole data provides a clearer understanding of the lithologic distribution and the boundary between the laterite and bedrock zones.

Keywords: Nickel Laterite; Electrical Resistivity Tomography (ERT); Borehole Data; Limonite Zone; Saprolite Zone.

Cite this as: Pahlawantika, I. O., Yatini, Y., & Wicaksono, M. A. 2025. Integration of Electrical Resistivity Tomography and Borehole Data for Mapping Laterite-Bedrock Boundaries in a Nickel Deposit, ‘Pho’ Block, Southeast Sulawesi. *IJAP: Indonesian Journal of Applied Physics, 15*(1), 176-192. doi: https://doi.org/10.13057/ijap.v15i1.93950

INTRODUCTION

Southeast Sulawesi, as one of the largest nickel laterite-producing regions in Indonesia, has a strategic position in the utilization and development of this resource The "PHO" Block is one of the potential prospected areas that need more development exploration of nickel laterite deposit. Exploring the resources included suggestions for prospected areas that play a crucial role in the region's resource utilization and development. Efficient exploration and accurate boundary delineation between laterite and bedrock are essential for effective mining planning and resource estimation. Mapping the boundary of lateritic soil and bedrock or fresh rock gives the price to the prospecting area, the main area, or the secondary area that needs to be developed step. However, mapping the bedrock boundary in nickel laterite deposits presents challenges due to complex subsurface lithological variations and differences in soil and rock physical properties [1]. Mapping bedrock boundaries in nickel laterite deposits is challenging due to complex subsurface lithologic heterogeneity and variations in soil and rock physical properties. The use of geophysical methods, such as ERT, has proven effective in identifying resistivity variations in the subsurface, which can illustrate the lithologic differences between laterite layers and bedrock[2].

Geophysical methods, particularly Electrical Resistivity Tomography (ERT), have been widely utilized to detect subsurface resistivity variations, aiding in lithological differentiation[3]. Previous studies in Sulawesi have explored nickel laterite deposits using various geophysical techniques. However, while ERT provides valuable resistivity-based insights, its interpretations require validation to ensure accuracy in delineating lithological boundaries. Borehole data, offering direct subsurface lithological information, serves as a crucial complementary method for verifying and refining ERT interpretations[4]. The integration of ERT and borehole data enables a more precise and comprehensive bedrock boundary mapping, facilitating informed decision-making in exploration activities and improving resource estimation accuracy [5].

Several previous studies on nickel laterite serve as both references and comparisons for the analysis conducted in this research. Arief (2023) integrated Electrical Resistivity Tomography (ERT) with geochemical analysis to map resistivity distribution and its correlation with iron oxide content [6]. Similarly, Suryawan [7] employed the Vertical Electrical Sounding (VES) method, successfully identifying nickel laterite deposits based on resistivity contrasts validated by borehole data. Meanwhile, Widyatmoko (2022) combined ERT and Ground Penetrating Radar (GPR) in North Konawe to enhance the accuracy of nickel laterite deposit mapping [2]. Building upon these studies, this research integrates ERT and borehole data to delineate the bedrock boundary in the "PHO" Block, Southeast Sulawesi. By refining lithological mapping accuracy, this study aims to address the specific challenges of exploration in this region while ensuring reliable subsurface characterization. The findings are expected to contribute not only to the advancement of data-driven exploration methodologies but also to the development of more efficient, sustainable, and environmentally responsible nickel laterite exploration strategies.

GEOLOGY OF THE RESEARCH AREA

Geologically, Southeast Sulawesi is located in the meeting zone between three major tectonic plates: the Indo-Australian Plate, the Eurasian Plate, and the Pacific Plate. This confluence causes tectonic solid activity, resulting in crustal deformation and the formation of metallic mineral deposits, including nickel laterite**.** The geological process resulted in 3 significant sections of Southeast Sulawesi regional stratigraphy (Figure 1):

- Continental Pieces
- Ofiolite Complex
- Molasa Sulawesi

The Pomalaa area is geologically located above the ultramafic rocks of the East Sulawesi Ofiolite with a dominance of Peridotite Serpentine) rocks [8]. The East Sulawesi Ofiolite complex is formed by tectonic processes, particularly at plate boundaries where oceanic plates are uplifted and accumulated into the continental crust. This process often occurs in subduction zones or mid-ocean ridges, where material from the seafloor is pushed upwards due to plate movement [8]. The morphology of the southeast arm of Sulawesi into five morphological units, namely mountain morphology, high hill morphology, low hill morphology, plain morphology, and karst morphology. The Pomalaa area is included in the Mendoke Mountain physiographic unit. The main controlling structures in the Pomalaa area of Kolaka consist of major fault systems, such as the Kolaka Fault (a strike-slip fault with a significant North-South direction of movement) and the Pomalaa Fault (a minor fault associated with the Kolaka Fault, oriented from northwest to southeast, with a similarly horizontal direction of movement), which influence the formation and distribution of nickel laterite deposits.

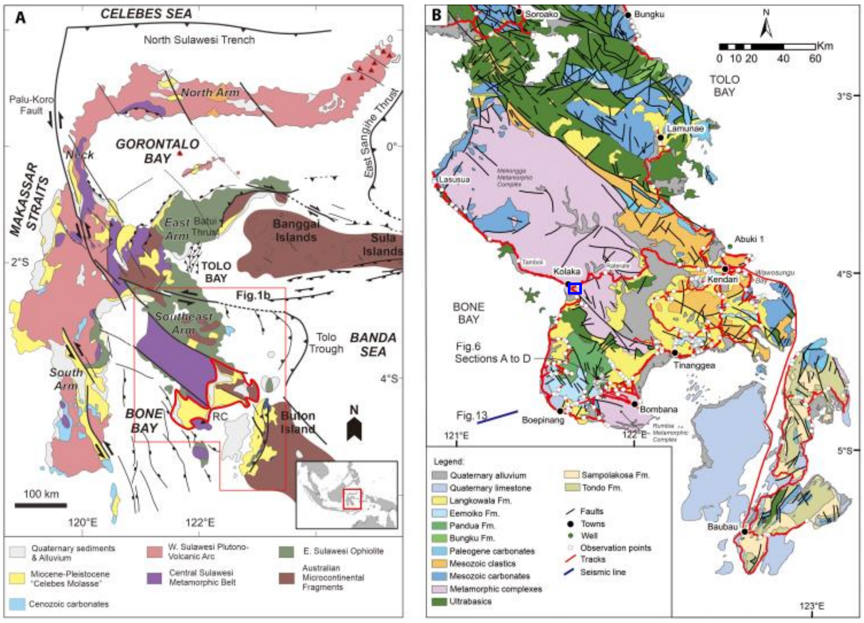

Figure 1. (a) Simplified geological map of Sulawesi by Hall and Wilson in [9], (b) Regional geological map of the study area [10]. The blue box shows the study area

Laterite deposits, also known as laterite deposits, result from intensive weathering processes that occur in areas with humid, warm or tropical climates. The weathering process results in the accumulation of clay minerals with kaolinitic properties and oxides/hydroxides of iron (Fe) and aluminum (Al). A distinctive feature of laterite deposits is the presence of well-defined layering, which results from the interaction between rainwater percolating into the rock formation and soil moisture rising to the surface. This process produces variable layers where mineral concentrations and physical characteristics of the soil can vary [1] . According the profile of laterite nickel deposits generally consists of several main zones, which are formed through weathering and laterization of ultrabasic or mafic rocks. The nickel laterite zone as shown in Figure 2. is divided into:

- Limonite Zone (Upper Laterite), This zone is located at the top of the laterite profile and is usually rich in iron oxides (Fe). The limonite consists of Goethite and Hematite, formed through intensive weathering. This zone has a lower nickel content than below but can contain significant Cobalt.
- The Saprolite zone, located below the limonite zone, consists of more Silicate-rich material with high Magnesium and Nickel content. Saprolite is formed from the weathering of primary minerals such as Olivine and Serpentine, but the original texture of the host rock can still be seen. Nickel in this zone is usually associated with Silicate minerals such as Garnierite.
- Saprock zone: this zone is a transition between the saprolite and bedrock zones. Basically, saprock is part of saprolite but still has the properties and characteristics of bedrock. This zone is part of saprolite in the form of coarse rocks and even boulders that have not undergone complete weathering.
- Bedrock zone, an ultrabasic rock that has not undergone significant weathering. This parent rock usually consists of Peridotite, Dunite, or Serpentinite.

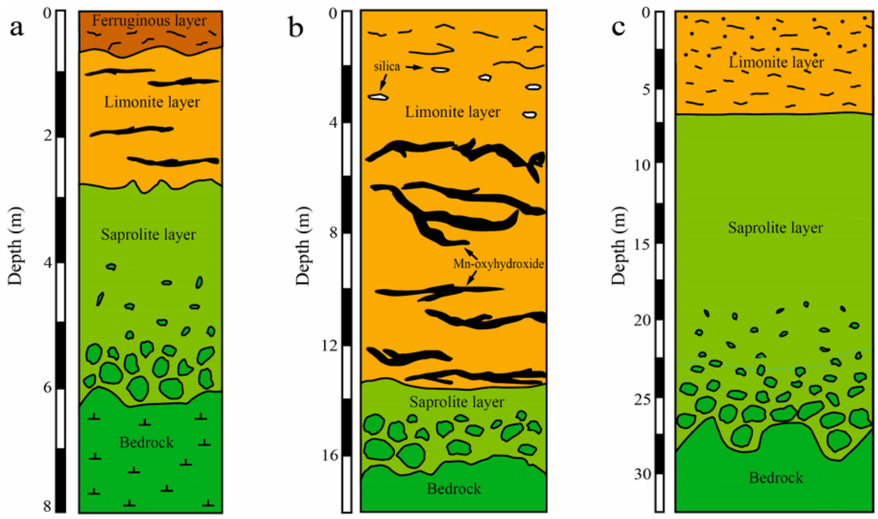

Figure 2. Schematic columnar sections of selected Ni(Co) laterite from (a) Indonesia (Kolonodale Ni deposit after), (b) the Philippines (Berong Ni-Co deposit after, and (c) Myanmar (Dagong shan Ni deposit after) [6]

METHODS

This study employs an integrated geophysical and geological approach to map the bedrock boundary in the "PHO" Block, Southeast Sulawesi. The methodology consists of data acquisition, data processing, and interpretation. The data acquisition phase involves Electrical Resistivity Tomography (ERT) and borehole drilling.

The ERT method generates electricity artificially, and the electric current is introduced into the soil, producing potential differences measured at the surface. The potential difference will generate information about the shape and electrical properties of the inhomogeneous subsurface components of the homogeneous soil [11]. The ERT method was conducted using a Dipole-Dipole configuration due to its high sensitivity to lateral variations, making it suitable for identifying laterite-bedrock boundaries.

The Dipole-Dipole configuration measurement uses 4 electrodes: a current electrode pair called 'current dipole C_1 C_2' and a potential electrode pair called 'potential dipole P_1 P_2 (Figure 3). In the Dipole-Dipole configuration, current and potential electrodes can be out of line and not symmetrical [9]. In this case the measured resistivity is apparent resistivity (ρ_a), hence the notion of specific resistance (resistivity/ρ) whose value is influenced by the installation of current and potential electrodes or geometry factors (k), the voltage read (V) and the current delivered (I). The apparent resistivity (ρ_a) can be calculated by multiplying the potential difference by the geometry factor (k) and dividing by the injected current:

$$\rho_a = k\frac{\Delta V}{I} \tag{1}$$

And the geometry factor (k) for the *dipole-dipole* configuration is:

$$k = \pi an(1+n)(2+n) \tag{2}$$

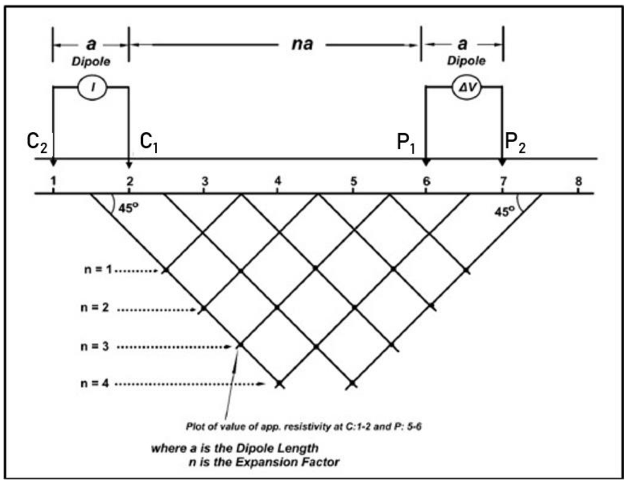

Figure 3. Schematic of pseudo section in modified Dipole-Dipole configuration[5]

The research is in the prospect area of PT Aneka Tambang Tbk Southeast Sulawesi. The data used in this study are primary data of the ERT method and full coring or sample borehole data. ERT acquisition in Block "PHO" with 8 ERT Lines with varying line lengths (Figure 4), optimized electrode spacing to enhance depth resolution. A multi-electrode resistivity system was used to improve accuracy. At the same time, the borehole data used was 23 borehole data (Figure 4), were drilled at selected locations to obtain direct lithological information, and core samples were analysed to validate resistivity-based lithological interpretations. ERT data acquisition uses MAE X612EM Multichannel Resistivitymeter as the main unit, with multichannel and single measurement features.

Data processing is divided into 3 stages: ERT data inversion, borehole data processing and analysis, and image processing to combine the analysis results of the two data. ERT data processing starts from primary field data to the results of the inversion of resistivity values. Inversion is the basis for making ERT data processing output from the model's data. Meanwhile, Borehole data processing is done by plotting drill points adjusted to collar data, lithology data, and survey data at each drill point. In addition, it also produces drill profiles based on drill and collar data supported by core box photos at that point, which is inline or on the ERT line. From the correlation of ERT and borehole data, further processing and analysis related to nickel laterite zone boundaries. Depth slices were analysed to distinguish resistivity contrasts between laterite and bedrock. Borehole data were then integrated with resistivity models to establish a resistivity-lithology relationship. Statistical analysis was performed to quantify the correlation between resistivity values and rock types. Advanced processing in the form of 3D distribution modeling using RockWorks software. The analysis involves all outputs from both ERT data processing, borehole data, and correlation of the two and is supported by previous research as reinforcement of interpretation.

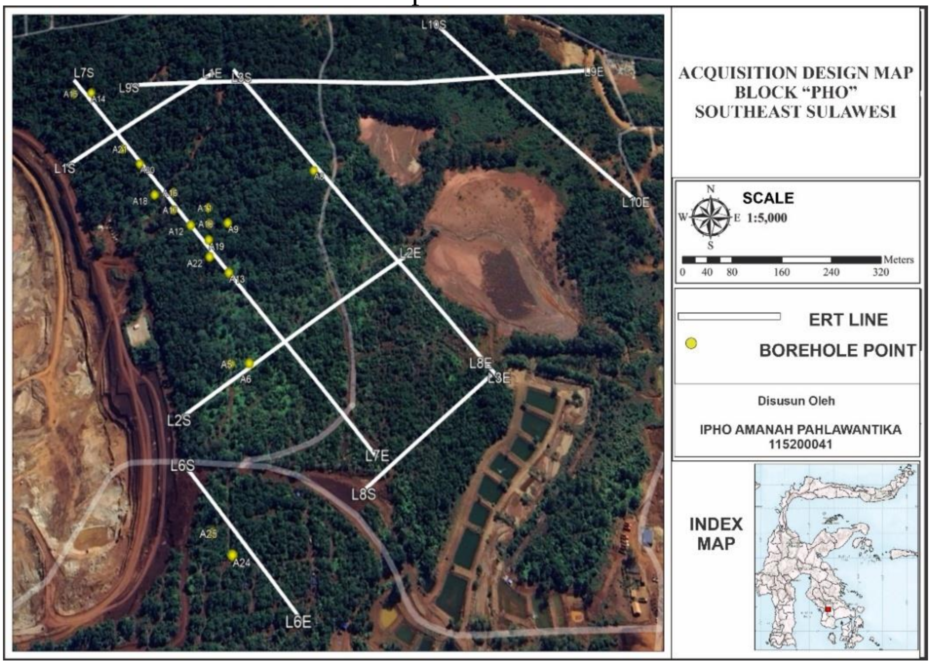

Figure 4. Acquisition design map of the study area and distribution of borehole data

The data processing phase involved ERT data inversion and lithological correlation. The collected resistivity data were processed using RES2DINV software to generate 2D resistivity models. Noise filtering and robust inversion techniques were applied to minimize errors and enhance subsurface imaging. Inverse modelling, or inversion, is an automated process where an algorithm iteratively compares measured data to a model's response [12] Since inversion does not yield a unique solution determining model accuracy can be challenging. A well-constructed model should be simple (following Occam’s principle), align with known ground properties (a priori information), and have minimal data misfit. However, simplicity can be interpreted in various ways, such as minimizing the number of layers or ensuring a smooth transition between model parameters.

The inversion routine used by the program is based on the smoothness-constrained least-squares method [2]. The inversion process starts with a basic homogeneous model, refining it through iterations to minimize the discrepancy between computed and observed resistivity values. This adjustment is governed by smoothness constraints and is quantified using the root-mean-squared (RMS) error. While a lower RMS error indicates a better fit, it does not always guarantee geological plausibility, as extreme resistivity variations may appear. Therefore, the best model is usually selected at the iteration where the RMS error stabilizes. Furthermore, the resistivity model to DAT, including resistivity value, coordinate, depth, and all data from the model. Next processing was built by Oasis Montaj for modelling the inversion value and integrating with the borehole data set.

The interpretation phase included bedrock boundary mapping and comparison with previous studies. The final interpreted bedrock boundary was delineated by correlating resistivity anomalies with borehole lithology. Discrepancies between ERT and borehole results were analysed, and possible causes were evaluated. A margin of error analysis was conducted to assess the accuracy of the interpreted boundary. The resistivity values obtained in this study were compared with those from similar nickel laterite deposits and deviations from expected resistivity ranges were examined, considering local geological variations.

The resulting correlation of ERT and borehole data produces values and responses regarding subsurface delineation. From these results, it is continued by reconstructing the data and outputs obtained into geological meanings that are by the conditions in the field. The interpretation used aims to obtain a section of inversion results which are then classified according to lithological interpretation. The results of the lithological classification are then integrated with borehole data to be used as a reference in determining the distribution of nickel laterite zones.

RESULTS AND DISCUSSION

This study integrates Electrical Resistivity Tomography (ERT) and borehole data to delineate the boundary between the laterite zone and bedrock. The ERT method processes resistivity values through RES2DINV software to generate 2D inversion sections, displaying the subsurface resistivity distribution. This resistivity variation is then classified into distinct lithological zones based on correlation with borehole data.

Classification of the resistivity value ranges of all passes was done by grouping the resistivity value categories against the subsurface lithological variations related to nickel laterite. The resistivity value range after grouping ranges from 10.86 Ωm to 1500 Ωm. The resistivity value category is divided into 4 resistivity value categories that indicate different lithologies (Table 1.).

Table 1. Classification of the range of resistivity values of the study area and interpretation of lithology based on the classification of the distribution of resistivity values of all passes

No	Classification	Resistivity Value (Ωm)	Lithology Interpretation
1.	Low	< 150	Saprolite
2.	Medium	150 – 700	Limonite
3.	High	700 – 1000	Saprock
4.	Very High	>1000	Bedrock/boulder

Based on the classification in (Table 1.) resistivity values below 150 Ωm are interpreted as a saprolite zone, which is formed due to intensive weathering so that this layer becomes a shaft and is dominated by refined grains to granules. Weathering in the saprolite zone is closely related to water, water fracture lines, and the water table, which play a role in the supergene enrichment process [13]. High water content leads to low resistivity because water is conductive and can conduct electric current.

The resistivity between (150-700) Ωm based on (Table 1.) is interpreted as the limonite zone, which has moderate resistivity and shows a lateral layering pattern. Due to the significant iron oxidation content, the resistivity value is higher than the saprolite zone [5]. However, there are lower resistivity anomalies when the limonite zone is associated with clays, Co compounds, and smectite minerals. Limonite zones associated with these components have different characteristics, resulting in lower resistivity compared to regular limonite zones. Above the limonite zone is a thin layer of topsoil (1-3 meters), rich in humus, iron oxidation, and shaft material, giving a value of medium to high resistivity. However, in this study, the topsoil is considered part of the limonite zone due to its thin thickness.The saprock zone, with a high resistivity between (700 – 1000) Ωm, based on the classification (Table 1.) is a transitional layer between saprolite and bedrock, dominated by fresh resistive boulder rocks but with conductive weathered layer, low moisture content with low to moderate weathering and serpentinization levels, and high fracture rates. Very high resistivity (>1000 Ωm) based on classification (Table 1.) indicates boulder or bedrock, which is fresh rock such as peridotite that has not been completely weathered. This bedrock originates from the eastern ophiolite complex in Southeast Sulawesi and is the main source of nickel laterite. The characteristics of bedrock when electrified are usually relatively dense and resistive with low water content relative to saprolite[5].

The resistivity classification in this study defines limonite within the range of 150 – 700 Ωm, saprolite below 150 Ωm, and bedrock exceeding 1000 Ωm. These values generally align with previous research in Pomalaa, particularly M. Arief W. (2023), which classified limonite within 181 – 800 Ωm, saprolite within 20 – 180 Ωm, and bedrock above 800 Ωm. However, slight differences in upper resistivity limits may be attributed to mineralogical variations, moisture content, or local geological conditions. In contrast, Eka H. S. (2019) reported significantly lower resistivity values, identifying lateritic soil within 5 – 55 Ωm and peridotite boulders between 56 – 170 Ωm, suggesting variations in weathering intensity and lithology between different blocks of Pomalaa. Similarly, Widyatmoko P. (2022) in North Konawe reported a higher limonite resistivity range (300 – 500 Ωm), likely due to higher iron oxide content and lower porosity, making the material more resistive.

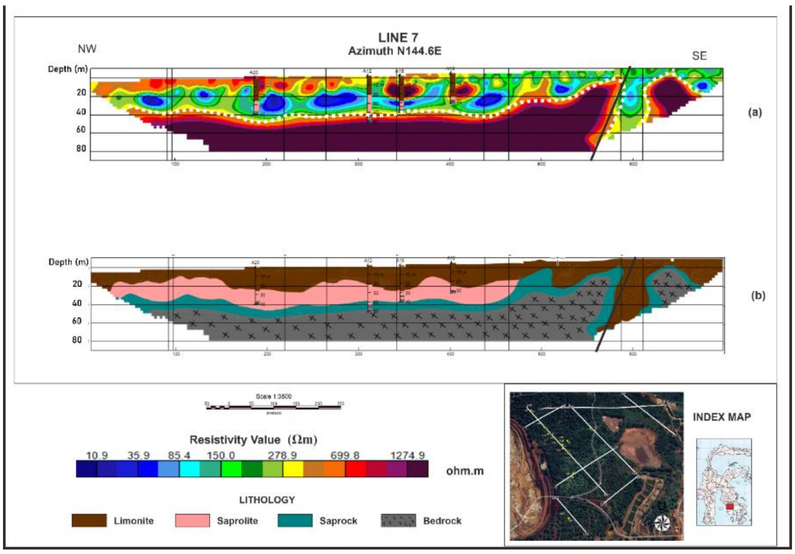

Figure 5. (a) 2D resistivity section and (b) lithology interpretation section of line 7. Dashed white line as bedrock boundary with laterite zone. The black line indicates the suspected weak zone.

Section of line 7 (Figure 5) has a line length of 710 meters with a spacing between electrodes of 10 meters, oriented Northwest-Southeast with an azimuth of N144.6 E. The distribution of resistivity values is low to very high with resistivity values of 10.9 Ωm to more than 1500 Ωm. In this section, the zone classification is based on the resistivity value response on the line with a range of values following Table 1. This trajectory shows the boundaries between zones of nickel laterite deposits that are quite clear and accompanied by the alleged existence of a weak zone indicated by the black line in Figure 5. The boundaries between these zones are generated based on the resistivity value response and analysis of the drill located on the trajectory as a reference zone boundary. A white dashed line indicates the boundary between the laterite zone and the bedrock.

The integration results between the lithology interpretation based on resistivity values and borehole data show a good match as shown in the inversion section and the lithology interpretation results in (Figure 5). The limonite zone with moderate resistivity is thickened in the center of the section, following the pattern of saprolite layers and undulating topography. The limonite zone does not spread across the entire section, only near the weak zone. The saprolite zone fills fractures in the Peridotite rock and shows low resistivity intersecting the high resistivity zone. The nickel laterite deposits on line 7 (Figure 5) show the response of the section following the undulations of the weathering of the Peridotite rocks with the limonite and saprolite layers thickening in the center of the section and at the top of the bedrock elevation. The depositional process followed fracture paths that allowed water to enter, causing physical and chemical weathering and mineral accumulation near the water table[14]. The weak zone is thought to have appeared after the deposition of nickel laterite, so the layers do not appear continuous.

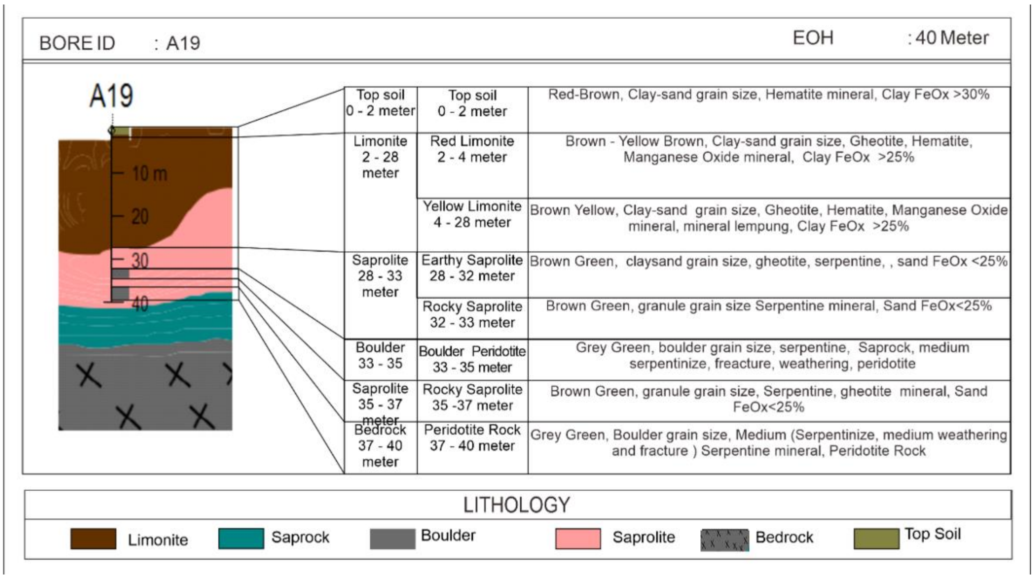

Figure 6. Example of profile of borehole result A19, there are 5-layer zones, including the *top soil* zone, *limonite* zone, saprolite zone, *bedrock* zone, and *boulder* logging description results from borehole result A19. From the results of the drill logging description, it is carried out macroscopically in the field and contains the drill depth, zone classification and thickness, to the minerals that appear in macroscopic observations.

The results of the integration of ERT interpretation and borehole analysis results show the similarity of the lithology present. Based on the results of the borehole analysis precisely at drill point A19 located on line 7 (Figure 6.), the analysis results show 5 zones namely top soil with a thickness of 2 meters, limonite with a thickness of 26 meters, saprolite with a thickness of 9 meters, boulder inserts with a total thickness of 2 meters, and bedrock at a depth of 37 meters, the total depth of this drill point or EOH 40 meters. When juxtaposed with the ERT interpretation results, the borehole analysis results show bedrock at a depth of 37 meters, while the lithological interpretation results show that at that depth it is still included in the saprolite lithology. The difference in results is possible that the results of the A19 borehole analysis which shows the presence of bedrock, are still in the saprolite lithology, however, the bedrock that is present is a saprock or silica boulder inserts in the saprolite zone, which if reviewed from the results of the borehole analysis at the depth above that shows the presence of boulder inserts at that depth. So, from the integration of the results of both the bedrock present is boulder and the actual bedrock is still below it.

The integration of ERT and borehole data revealed a strong correlation in approximately 80% of cases, yet some discrepancies were observed in lithological boundary depths and resistivity classifications. The margin of error in this study was calculated at ±1.5 meters, influenced by several key factors. One primary cause is the overlap of resistivity values between lithologies, particularly in the transition between saprolite and limonite, where gradual weathering results in resistivity variations that make precise boundary delineation difficult. Additionally, moisture content fluctuations affect resistivity values, as higher groundwater saturation leads to increased conductivity, potentially shifting the interpreted boundary positions in ERT models.

Another factor contributing to discrepancies is the resolution limitations of ERT, where deeper layers experience greater uncertainty due to signal attenuation and a decrease in sensitivity to small-scale variations. This can lead to misinterpretation of buried boulders or compacted saprolite as bedrock, causing variations in boundary depth estimations between ERT and borehole data. Borehole analysis confirmed laterite thickness variations from 20 to 49.9 meters, generally supporting ERT interpretations, but in some areas, ERT suggested a deeper bedrock boundary than indicated by borehole data. This discrepancy is likely due to heterogeneous weathering patterns, where certain areas contain partially weathered peridotite or saprock zones that exhibit intermediate resistivity values, leading to classification differences.

While the overall correlation between ERT and borehole data was strong, some inconsistencies were observed in specific locations. In several borehole points, ERT indicated a deeper saprolite-bedrock boundary than borehole observations, suggesting that resistivity values may not always provide a clear separation between saprolite and bedrock. This discrepancy is likely due to partially weathered peridotite or saprock layers, which exhibit intermediate resistivity values, leading to classification differences between the two methods. Additionally, in certain areas where borehole data identified compacted boulders or saprock, ERT misinterpreted these as bedrock due to their higher resistivity values. Moisture content also played a significant role in influencing resistivity values. Areas with higher groundwater saturation exhibited lower resistivity, causing ERT to misclassify certain saprolite layers as limonite due to increased conductivity. Conversely, dry, compacted zones with high iron oxide content exhibited resistivity values similar to bedrock, making it difficult to distinguish them from underlying unweathered peridotite.

Cross-sectional correlations of all the passes (Figure 7) show a consistent continuity of resistivity values in the intersecting areas, with a continuous contrast of high and low resistivity between the passes reflecting the presence of weak zones due to geological structures. This weak zone is characterized by low resistivity intersecting continuous high resistivity. However, at the end of the trajectory, this continuity pattern is less clear because there are no intersecting trajectories, so further study is required. The pattern of high resistivity suspected to be bedrock is thicker in high topographic areas and thins in steep areas, following the local morphology.

The thickening of the laterite layer is dominant to the east-north direction, while the bedrock forms an elevation to the west-northwest direction, influenced by geological structures. In the "PHO" Block, suspected faults are visible in several passes. The low resistivity value in the near-surface area is thought to be due to the presence of a river branch, which is located on the measurement line.

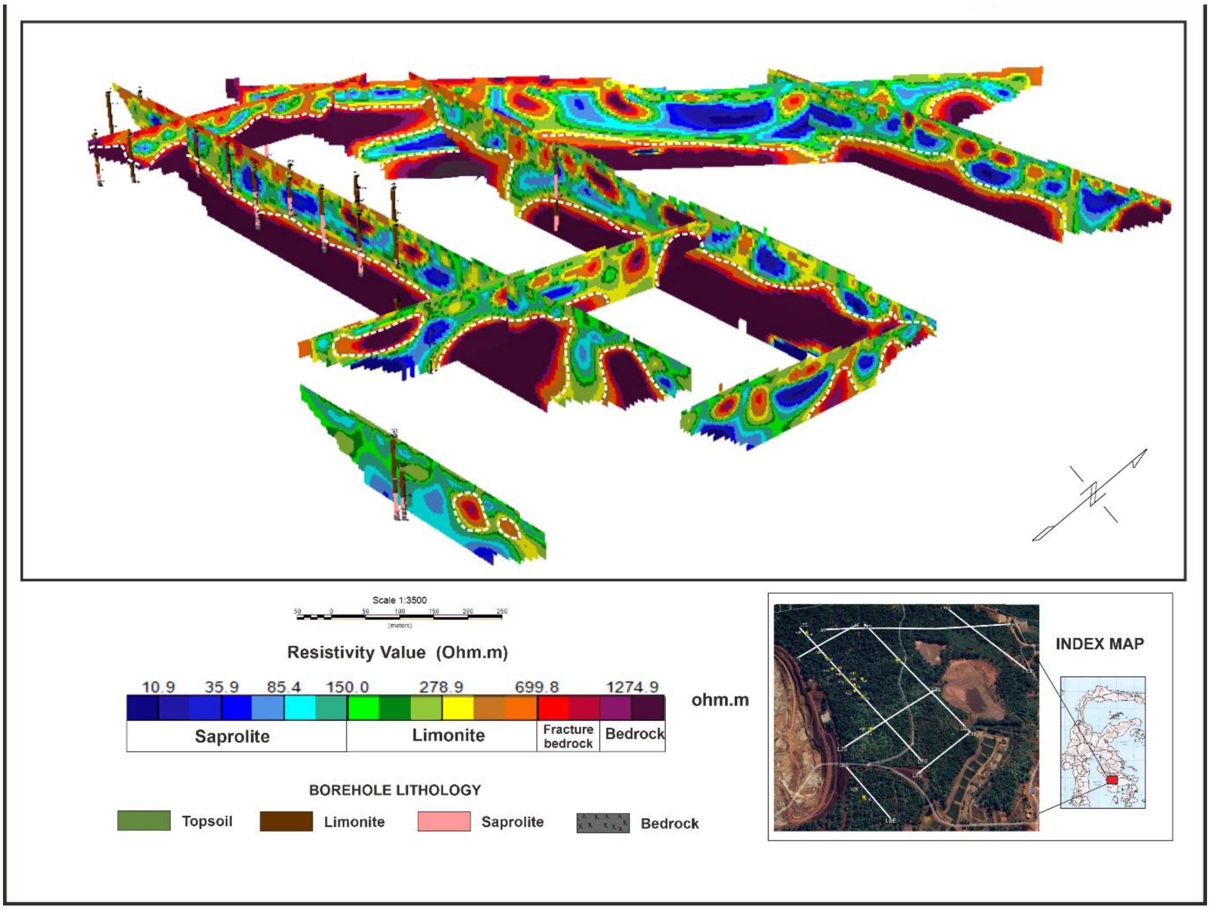

Figure 7. Correlation of resistivity section of inversion results of all south - north oriented trajectories. The boundary between the laterite zone and bedrock is indicated by a white dashed line. The black line indicates the suspected weak zone.

The boundary between the laterite zone and bedrock is quite visible in the resistivity section correlation. The boundary between the two is indicated by a white dashed line that shows its continuity on each line. However, lines 6 and 8 are less visible for the massive shape of the bedrock. The two passes are known to have a shallower depth when compared to the other passes, so the presence of bedrock has not appeared on the two passes. Both passes show the presence of boulders or the presence of saprock with a response to form a closure with high - very high resistivity values.

The depth slicing map shows resistivity variations at depths of 6.8 meters, 31.9 meters, 21.5 meters, and 49.9 meters, illustrating the distribution of nickel laterite lithology shown in (Figure 8.). At a depth of 6.8 meters, a layer of topsoil with high resistivity was identified in the northwest, while low resistivity was seen in line 9 due to the river and in the east due to the flow of the dam. Limonite appears at this depth with an even distribution in the "PHO" Block. At further depths, the high resistivity is suspected to be the limonite layer below the topsoil, with the same pattern. Resistivity variations in the limonite layer indicate differences in mineral content[5].

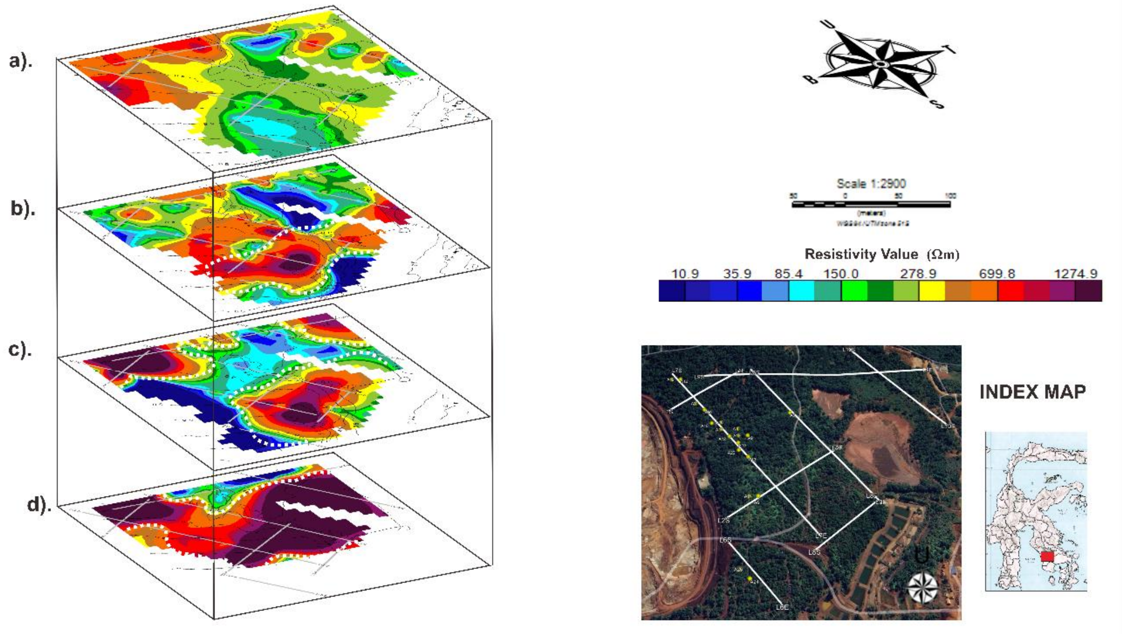

Figure 8. Depth slicing map (a) 6.8 m, (b) 21.5, (c) 31.3 m and (d) 49.9 m.

Slicing maps of depths of 6.8 meters to 21.5 meters show significant changes in the responses generated. This shows a zone change based on the response displayed. At a depth of 6.8 meters shows the presence of limonite and saprolite, in contrast to a depth of 21.5 meters which begins to show a high - very high resistivity value response which is thought to be boulder or saprock. Bedrock/boulder to saprock begins to dominate at 21.5 meters depth, especially in traverses 7, 3, 6, and 2, with saprolite layers at the top. The presence of boulder to saprock at this depth is seen when at a further depth it shows continuity in some areas which is thought to be a continuation of the presence of bedrock, and in some areas, it does not show continuity indicating that the area is boulder to saprock. At a depth of 31.3 meters, saprock and bedrock dominate, with saprolite beginning to narrow at the top of the map. Areas that show continuity from the previous depth can be assumed to be bedrock areas. The 49.9-meter depth is dominated by bedrock, but saprolite is still found in some areas. At this depth, it shows the bedrock boundary and laterite zone in some areas. However, on passes 6 and 8 it does not show a response because the pass is quite shallow and does not reach that depth. Based on the borehole result, the saprolite layer is generally located at more than 20 meters, while limonite appears from a shallow depth of approximately 21.5 meters on the depth-slicing map. Limonite layer thickness is greater than saprolite, and the dominant saprock-bedrock zone ranges from 21.5 to 49.9 meters. The results show differences in layer thickness in some areas so that the boundaries between the laterite zone and bedrock in certain areas have differences, where the laterite nickel deposition process is strongly influenced by sloping topography, where the accumulation of deposits tends to occur in flat areas.

In Block "PHO" (Figure 9), the distribution of the reddish-brown limonite zone is quite thick in the south and thin in the northwest and east of the map. The distribution model shows that the limonite zone starts to appear from the surface to the bottom of the model. The thickness of the limonite zone is influenced by the resistivity value on each line, with greater thickness in the south and northeast areas. The formation of nickel laterite deposits in this area is the result of complex interactions between ultramafic host rocks, intensive chemical weathering, and local geological and topographic conditions [15]. The study area, located in a tropical climate with high rainfall and constant temperatures throughout the year, accelerates the chemical weathering process. Acidic rainwater decomposes minerals in ultramafic rocks, and varied topography, such as hills and plateaus, plays an important role in the formation of nickel laterite [16]. In higher areas, the weathering of ultramafic rocks is more intensive, resulting in thicker limonite and saprolite. Geologically, the formation of nickel laterite deposits shows the complexity of tectonic activity that influenced the depositional pattern in the study area. The deposition pattern of nickel laterite tends to be centered on more sloping areas with thicker limonite thickness.

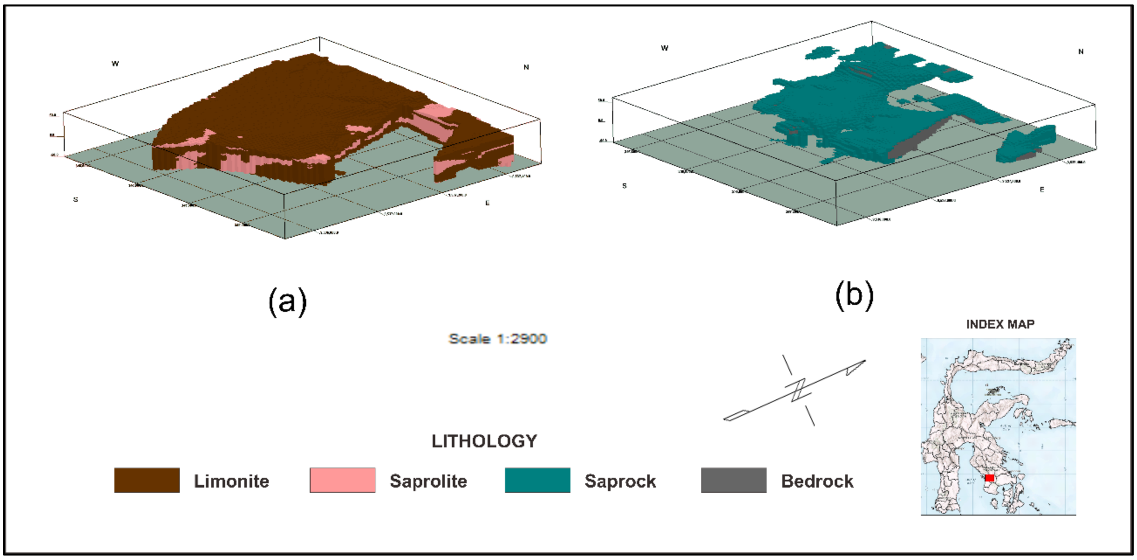

Figure 9. 3D modeling of the distribution of (a) laterite zone (limonite and saprolite) (b) saprock and bedrock of the study area based on the classification of resistivity values in Table 1**.**

The distribution of the saprolite zone is more dominant in the south and north (Figure 9), with greater thickness than the thinner central part of the model. More intense and longer-lasting weathering processes produce thicker saprolite, while less intense weathering produces thinner saprolite. Other factors such as rapid groundwater flow or a good drainage system may accelerate the leaching of minerals from the saprolite layer, resulting in a thinner layer [11]. In the "PHO" Block, the river flow from the southeast to the northeast also affects the thickness of the saprolite. The saprock and bedrock zones show similar distribution patterns, where the saprock is a highly fractured transition that has not undergone complete weathering, while the bedrock shows deeper weathering. Both are dominant in the central and northwestern parts with varying thicknesses. The difference in bedrock thickness is closely related to the presence of faults or cracks that accelerate the weathering and thinning of the bedrock. Geological structures such as faults and folds can affect bedrock thickness by creating weak zones that accelerate weathering and uplift rock units [11].

The results of the scatter and drill model show that the bedrock is more dominant in the central and northwest to southeast sections with varying thicknesses. The scatter results show the boundary between the bedrock and laterite zones in certain areas. The scatter results show the dominance of the laterite zone and the bedrock zone covered by saprock. Overall, the distribution of the nickel laterite zone is strongly influenced by the morphology of the area, with the thickness of the limonite zone being greater in sloping areas and thinning in steeper areas. The thickening of the saprolite zone also follows topography and river flow, with the steeper the area, the thinner the deposition.

The distribution of the limonite zone, characterized by its reddish-brown color, is notably thick in the southern part of Area A but becomes thinner in the northwest and eastern regions. The distribution of lateritic nickel zones is strongly influenced by the area's topography. Based on the resistivity values and 3D zonation in Area A, the distribution of lateritic nickel deposits aligns with the morphology of the study area, influenced by mineral composition, particularly iron oxides and silica content, which affect resistivity responses. The thickest limonite zone is concentrated in the northern and northeastern parts, where the terrain is more level. Meanwhile, the saprolite zone thickens in similar areas but becomes thinner near the central region, which corresponds to a river flow area. The steeper the terrain, the thinner the deposit accumulation.

The geological structure plays a crucial role in nickel laterite formation and distribution. The undulating topography and faulting in the PHO Block have significantly influenced laterite accumulation. Weak zones identified in the ERT sections indicate possible fault-related fractures, which facilitated groundwater infiltration, enhancing chemical weathering and laterization. These fractures promote water flow, enriching the limonite and saprolite zones by leaching primary ultramafic minerals and concentrating nickel-bearing minerals such as Garnierite and Goethite.

Topographical and structural influences play a significant role in resistivity variations. According to previous research by Eka H. S. (2019)[7], the limonite zone was relatively thin and could not effectively separate it from the saprolite zone, leading to their combination. However, in Block A, the limonite zone is significantly thicker than the saprolite zone. Although the study by Eka H. S. (2019)[7] was conducted in the same general area, it focused on a different block or hill, which could explain the variations in the lateritic nickel deposit formation. The thicker limonite zone in the PHO Block compared to Eka H. S. (2019)[7] suggests lower erosion rates and more stable lateralization, whereas the nickel laterite distribution aligns with local morphology, similar to M. Arief W. (2023)[5]. The results indicate that flatter areas promote greater limonite accumulation, while steeper slopes show thinner deposits due to erosion and reduced material retention. Weak zones detected in ERT suggest fault-related fractures that facilitated groundwater infiltration, mineral leaching, and chemical weathering, contributing to nickel enrichment in the limonite and saprolite zones.

The study reveals that topography and drainage patterns significantly affect laterite deposition. Thicker laterite accumulations are observed in low-lying areas, whereas steeper slopes tend to exhibit thinner deposits due to increased erosion and lower retention of weathered material. This finding aligns with previous studies on nickel laterite deposits in ultramafic terrains, confirming the importance of slope stability and hydrology in laterite formation. Moreover, the integration of 3D geological modelling with ERT and borehole data provides a clearer visualization of the laterite-bedrock boundary. The findings suggest that nickel laterite deposits in the PHO Block predominantly follow tectonic lineaments, emphasizing the need for further geophysical exploration along suspected fault zones to delineate additional resource potential.

To improve lithology-resistivity correlation, future studies should integrate geochemical validation to refine resistivity-based interpretations, particularly in transition zones between saprolite and bedrock. Additionally, using complementary geophysical methods such as Induced Polarization (IP), which is more sensitive to mineral composition, or Ground Penetrating Radar (GPR), which provides high-resolution near-surface imaging, could help differentiate lithological boundaries with greater accuracy. Advanced inversion techniques, including machine learning-assisted resistivity classification, could also enhance model reliability and reduce interpretation errors in nickel laterite exploration.

CONCLUSIONS

The 2D inversion results show the distribution of resistivity values in the "PHO" Block with a range from 10.86 Ωm to 1500 Ωm. which is divided into 4 zones based on resistivity values: saprolite zone with resistivity value <150 Ωm, limonite zone with resistivity value (150 – 700) Ωm, saprock or boulder zone with resistivity value (700 – 1000) Ωm, and bedrock zone with resistivity value >1000 Ωm. The boundary between laterite deposit zones is based on the depth of each zone, the limonite zone with a thickness of more than 20 meters and is evenly distributed throughout the "PHO" Block at shallow depths to more than 20 meters. The saprolite zone, with an average thickness of less than 20 meters, is thinner than the limonite zone and is found at depths of more than 20 meters. The bedrock boundary with the laterite zone is visible at a depth of 31.1 meters in some areas to a depth of 49.9 meters evenly except in the north to Southeast area which is more than 49.9. The distribution characteristics of nickel laterite zones in the "PHO" Block show the dominance of thick limonite zones in the northeast and south areas. The saprolite zone is quite thin in the central part and concentrated in the south and north. The saprock and bedrock zones are thicker in the northwest to central part of the area.

REFERENCES

1. Kamaruddin, H., Indrakususma, R. A., Rosana, M. F., Sulaksana, N., & Yuningsih, E. T. (2018). Profil Endapan Laterit Nikel Di Pomalaa, Kabupaten Kolaka, Provinsi Sulawesi Tenggara. *Buletin Sumber Daya Geologi*, *13*(2), 84-105.
2. Loke, M. H. 2004. Tutorial: 2-D and 3-D electrical imaging surveys. Online: www.geoelectrical.com
3. White, R. E. 2016. Geophysical and geochemical integration for mapping nickel laterite deposits. *Geophysics, 81*(5), B179–B188.
4. Dahlin, T. 2001. The development of DC resistivity imaging techniques. *Computers & Geosciences*, *27*(9), 1019-1029.
5. Wicaksono, M. A., Mordekhai, D. S., & Rahmat, A. S. 2023. Integrating Resistivity and Geochemical Component Data with Bayesian Inference to Characterize Nickel Laterites: A Case Study from Pomalaa Region Using Large-Scale Borehole Data. *hand*, *23*, 26th.
6. Soh Tamehe, L., Zhao, Y., Xu, W., & Gao, J. 2024. Ni (Co) Laterite Deposits of Southeast Asia: A Review and Perspective. *Minerals*, *14*(2), 134.
7. Suryawan, E. H., Hilyah, A., Fajar, M. H. M., & Pajrin, A. 2019. Identifikasi Dan Penentuan Volume Endapan Nikel Laterit Berdasarkan Data Geolistrik Metode Sounding Studi Kasus Blok Selatan Daerah Pomalaa, Sulawesi Tenggara. *Jurnal Geosaintek*, *5*(2), 53-60.
8. Ministry of Energy and M. Resources. 2020. *Indonesia's Nickel Resources*.
9. Nugraha, A. M. S., Hall, R., & BouDagher-Fadel, M. 2022. The Celebes Molasse: A revised Neogene stratigraphy for Sulawesi, Indonesia. *Journal of Asian Earth Sciences*, *228*, 105140.
10. Nugraha, A. M. S., Hall, R., BouDagher-Fadel, M., Todd, J. A., & Switzer, A. D. 2023. Neogene history of fluvial to shallow marine successions in the Kendari Basin, SE Sulawesi, Indonesia. *The Depositional Record*, *9*(2), 300-334.
11. Aswad, S., & Mais, D. M. 2018. ERT and Well Data Tie for Nickel Laterite Characterization. In *IOP Conference Series: Earth and Environmental Science*, 132(1), 012024. IOP Publishing.
12. Hellman, K., Johansson, S. J., Olsson, P. O., & Dahlin, T. D. 2016. Resistivity inversion software comparison. In *Near Surface Geoscience 2016-22nd European Meeting of Environmental and Engineering Geophysics*, 2016(1), cp-495). European Association of Geoscientists & Engineers.
13. Putri, H. S. 2023. *Identifikasi persebaran mineral silika menggunakan metode geolistrik konfigurasi pole-dipole dengan pemodelan 2d kota kolaka, sulawesi tenggara* (Bachelor's thesis, Fakultas Sains dan Teknologi UIN Syarif HIdayatullah Jakarta).

14 Masri, M., Mili, M. Z., Awaliah, W. R., Tugo, L. J., & Rifai, L. A. 2023. Mineralogi dan Properti Keteknikan Endapan Nikel Laterit Daerah Tobimeita-Langgikima, Kabupaten Konawe Utara, Sulawesi Tenggara. *Jurnal GEOSAPTA*, *9*(2), 117-125.

15 Maulana, A. 2017. *Endapan Mineral*. Universitas Hassanudin.

16 Zhang, Y., Qie, J., Wang, X. F., Cui, K., Fu, T., Wang, J., & Qi, Y. 2020. Mineralogical characteristics of the nickel laterite, southeast ophiolite belt, Sulawesi Island, Indonesia. *Mining, Metallurgy & Exploration*, *37*(1), 79-91.